JOURNAL OF AIRCRAFT
Vol. 38, No. 1, January–February 2001

Wing Rock of Nonslender Delta Wings

Lars E. Ericsson*
Mountain View, California 94040

That slender delta wings will experience wing rock is an established fact, and the responsible flow mechanism is well understood. However, the same flow mechanism could not cause wing rock of nonslender delta wings. Thus, the wing rock observed for a 45-deg delta wing must be generated by a different flow phenomenon. Experimental results for delta wings and airfoils are analyzed in order to define the flow mechanism driving the observed wing-rock motion.

Nomenclature

b	=	wing span
c	=	wing root chord
f	=	oscillation frequency
K	=	reduced roll rate, $b\dot{\phi}/2U_\infty$
L	=	lift: coefficient $C_L = L/(\rho_\infty U_\infty^2/2)S$
L'	=	two-dimensional lift: coefficient $c_l = L'/(\rho_\infty U_\infty^2/2)c$
l	=	rolling moment: coefficient $C_l = l/(\rho_\infty U_\infty^2/2)Sb$
M	=	Mach number
Re	=	Reynolds number based on c and freestream conditions
S	=	reference area; projected wing planform area
t	=	time
U	=	horizontal velocity
x	=	chordwise, body-fixed coordinate ($x_{LE} = 0$)
z	=	vertical displacement
α	=	angle of attack
β	=	angle of sideslip
Δ	=	amplitude
ζ	=	dimensionless z coordinate, z/c
θ_{LE}	=	apex half-angle, $\theta_{LE} = \pi/2 - \Lambda$
Λ	=	leading-edge sweep
ξ	=	dimensionless x coordinate, x/c
ρ	=	air density
σ	=	inclination of the roll axis
ϕ	=	roll angle
ω	=	angular oscillation frequency, $2\pi f$
$\bar{\omega}$	=	reduced frequency, $\omega c/U_\infty$

Subscripts

B	=	vortex breakdown
cr	=	critical
d	=	discontinuity
eff	=	effective
LE	=	leading edge
s	=	stall
v	=	vortex shedding starts
0, 1	=	numbering subscript
∞	=	freestream conditions

Introduction

A RECENT publication[1] pointed out that, although the wing rock problem for slender delta wings has been investigated extensively,[2] the possibility that a similar problem could exist for nonslender delta wings has been ignored, in spite of the fact that many existing and planned future aerospace vehicles incorporate this wing planform. Although vortex-induced loads dominate on slender delta wings, causing the observed wing rock,[2] they play no significant role in generating the nonslender wing rock phenomenon of the present 45-deg delta wing. However, an important consideration for these wings is that they have large leading-edge radii, rather than being sharp-edged, as in the case of the configurations exhibiting slender wing rock. As a representative configuration for investigation of the low-speed aerodynamics of an aerospace plane during the landing approach, the authors of Ref. 1 selected a thick 45-deg delta wing with cylindrical leading edges (Fig. 1).

Discussion

Low-speed tests at $Re = 0.22 \times 10^6$ of a 45-deg delta wing[1] (Fig. 1) gave a maximum lift close to that for a NACA-0012 airfoil[3] (Fig. 2). At $\alpha < 10$ deg the lift slope of the delta wing is roughly 60% of that for the airfoil. Correcting for the effect of aspect ratio (AR) and assuming elliptic lift distribution, one obtains $C_{L\alpha} = c_{l\alpha}/(1 + c_{l\alpha}/\pi\,\mathrm{AR})$, giving $C_{L\alpha}/c_{l\alpha} = \frac{2}{3}$ for $c_{l\alpha} = 2\pi$ and AR$= 4$. Thus, at $\phi = \beta = 0$ the $C_L(\alpha)$ characteristics of the 45-deg delta wing are similar to those for a straight wing. Applying the stall angle α_s for the NACA-0012 airfoil to the crossflow separation angle α_{LE} on the delta wing gives the angle of attack α_v for starting vortex shedding as follows[4]:

$$\alpha_v = \tan^{-1}(\tan\alpha_{LE}\sin\theta_{LE}) \tag{1}$$

With $\alpha_{LE} = \alpha_s = 11$ deg for NACA-0012 (Fig. 2) and $\theta_{LE} = 45$ deg (Fig. 1), Eq. (1) gives $\alpha_v = 8$ deg. The experimental results in Fig. 2 indicate that the leading-edge stall occurred at $\alpha_v \approx 10$ deg, compared to $\alpha \approx 12$ deg for the NACA-0012 airfoil, resulting in leading-edge vortex shedding at $\alpha - \alpha_v > 0$. Based upon the straight-wing type of $C_L(\alpha)$ behavior up to maximum lift at $\alpha = 25$ deg (Fig. 2), one expects the delta wing to exhibit symmetric rolling moment characteristics, $C_l(-\phi) \approx C_l(\phi)$ at inclinations $\sigma < 25$ deg of the roll axis below wing stall, in basic agreement with the measured $C_l(\phi)$ characteristics at $\sigma = 10$ deg (Fig. 3). At $\alpha \approx 25$ deg, where the lift for $\phi = \beta = 0$ has reached its maximum value $C_{l\,max} = 1.0$ (Fig. 2), vortex breakdown should have started to occur according to experimental results[5] (Fig. 4). Although the pertinent flow phenomenon for the 45-deg delta wing is the part-span vortex shedding[6,7] (Fig. 5), rather than vortex breakdown (Fig. 4), both produce similar results, i.e., a loss of the vortex lift generated on the outboard, aft wing area.

The effective leading-edge sweep of the right and left wing halves changes as follows[2] with the roll angle ϕ and inclination σ of the roll axis:

$$\Lambda_{eff} = \Lambda \pm \tan^{-1}(\tan\sigma\sin\phi) \tag{2}$$

For $\Lambda = 45$ deg Eq. (2) gives $\Lambda_{eff} = 60$ deg for the leeward, rising wing-half at $\phi \approx 28$ deg for $\sigma = 30$ deg and at $\phi \approx 35$ deg for $\sigma = 20$ deg. On the opposite, dipping wing-half $\Lambda_{eff} = 30$ deg. As the tests covered $-90\ \mathrm{deg} \le \phi \le 90$ deg, it is expedient to let the vortex breakdown phenomenon generate the loss of vortex lift resulting as the effective leading-edge sweep of the two wing halves

Presented as Paper 00-0137 at the 38th Aerospace Sciences Meeting and Exhibit, Reno, NV, 11–13 January 2000; received 10 February 2000; revision received 10 July 2000; accepted for publication 12 July 2000.

*Engineering Consultant. Fellow AIAA.

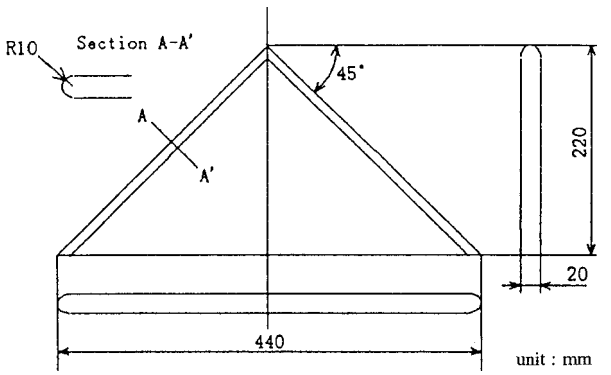

Fig. 1 Nonslender delta wing model.[1]

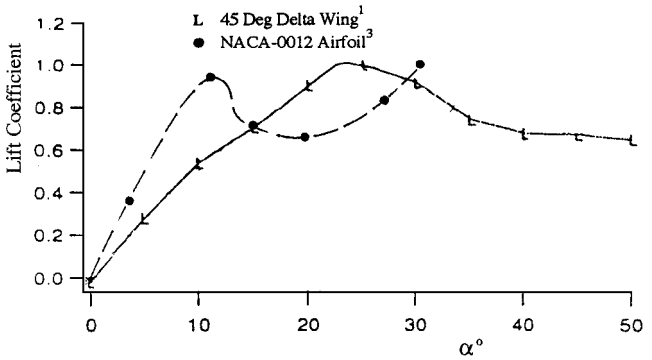

Fig. 2 Lift coefficients of 45-deg delta-wing model and NACA-0012 airfoil.

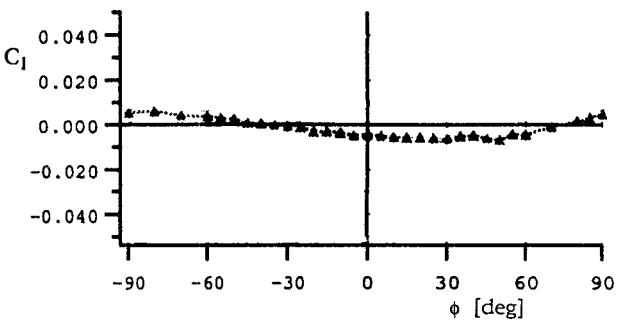

Fig. 3 $C_\ell(\phi)$ at σ = 10 deg of 45-deg delta-wing model.[1]

varies with the roll angle. This is justified based on the fact that Λ_{eff} will in both cases have a similar effect on the loss of vortex lift on the outboard wing panel (Figs. 4 and 5). The experimental results[1] in Fig. 6 for $\sigma = 25$ and 30 deg are dominated by the vortex-induced loads on the rising, leeward wing half. Consequently, they display the antisymmetric $C_l(\phi)$ characteristics $C_l(-\phi) = -C_l(\phi)$ expected from the roll-induced opposite changes of the vortex-induced loads on the two wing halves, through the change of Λ_{eff} described by Eq. (2).

The results for $\sigma = 30$ deg (Fig. 6b) are very similar to those for $\sigma = 30$ deg of a 65-deg delta-wing-body configuration[8,9] (Fig. 7). In both cases there are three trim points $\phi_0 \approx 0$ and $\pm\phi_1 \neq 0$. As discussed in Ref. 10, the measured $C_l(\phi)$ characteristics, although being highly nonlinear, are continuous, not discontinuous as in the IDEALIZATION approximation in Fig. 7. At $|\phi| < \phi_{cr}$ the full vortex-induced lift forward of breakdown and the lift generated by the helical flow downstream of a spiral vortex breakdown[11] combine to generate a statically stabilizing rolling moment contribution on the windward wing half that overpowers the corresponding statically destabilizing rolling moment generated by the downstream movement of vortex breakdown on the leeward side. This is a result of the change of effective leading-edge sweep associated with the nonzero roll angle, Eq. (2). As a consequence, $\phi = 0$ is a stable trim point

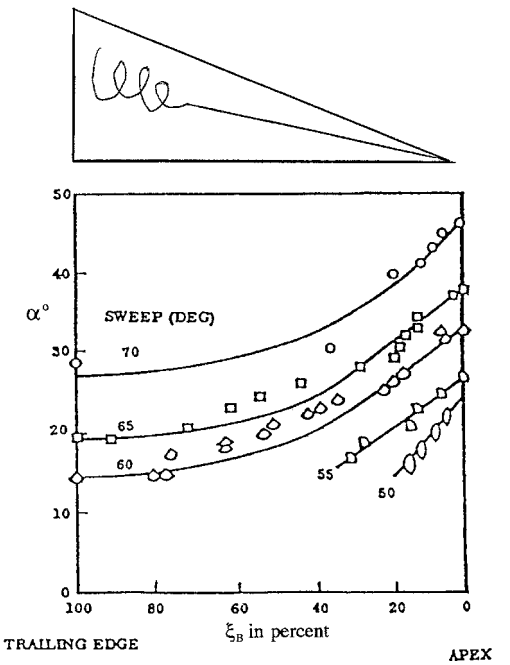

Fig. 4 Effect of leading-edge sweep on vortex breakdown location for sharp-edged delta wings.[5]

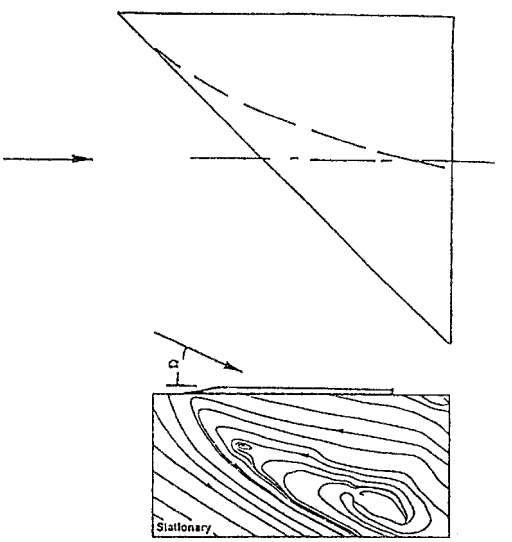

45-deg delta wing at α = 30 deg[6]

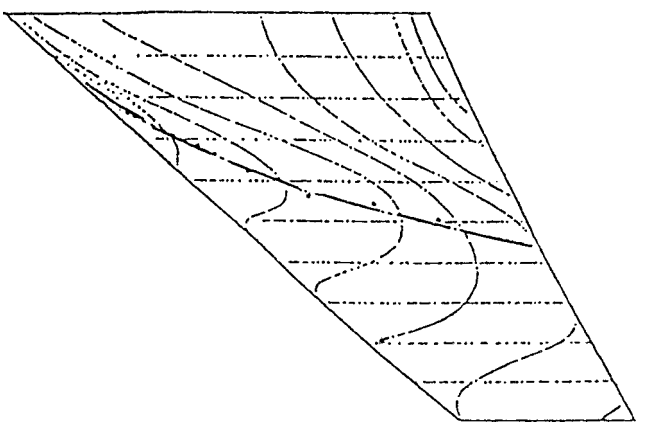

49.4-deg cropped arrowhead wing at α = 20 deg[7]

Fig. 5 Partial span vortex characteristics.

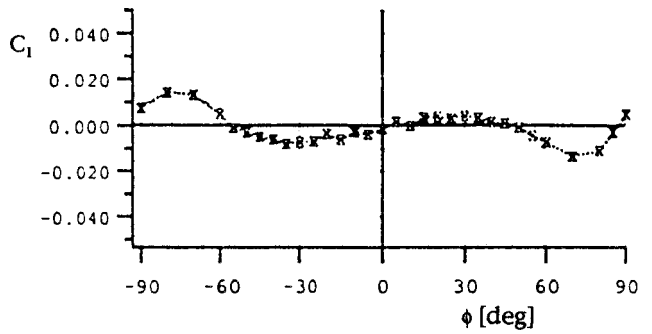

a) σ = 25 deg

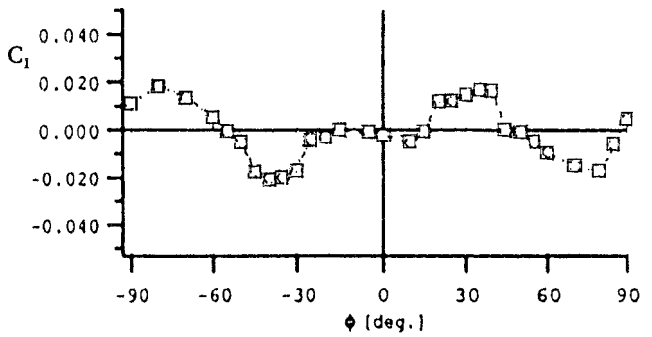

b) σ = 30 deg

Fig. 6 $C_\ell(\phi)$ **of 45-deg delta-wing model.**[1]

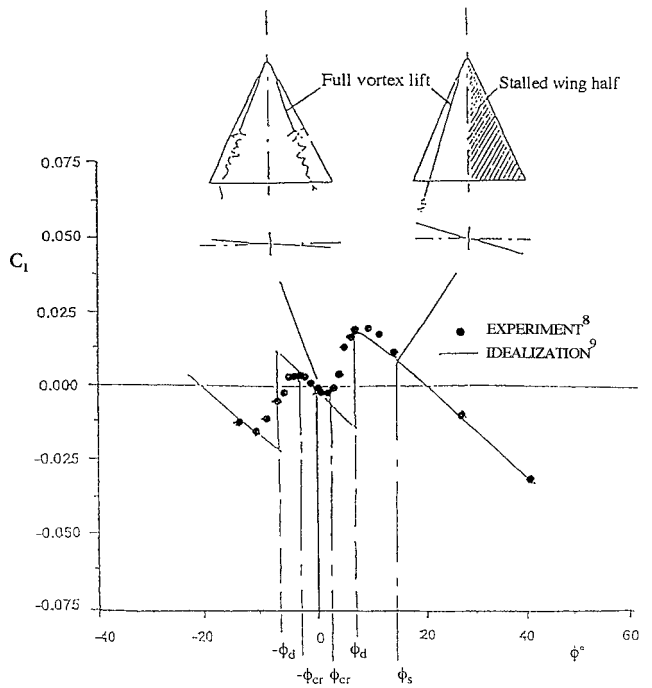

Fig. 7 $C_\ell(\phi)$ **at** σ **= 30 deg of 65-deg sharp-edged delta-wing-body configuration.**[8,9]

for $|\phi| < \phi_{cr}$ (Fig. 7). When $|\phi| > \phi_{cr} \approx 4$ deg, vortex breakdown moves very rapidly toward the trailing edge on the leeward, rising wing half. The associated rapid increase of the statically destabilizing vortex-induced lift overpowers the statically stabilizing data trend from the lift generated by vortical and helical flow on both wing halves,[9–12] resulting in the measured statically destabilizing $C_l(\phi)$ trend for $\phi_{cr} < |\phi| < \phi_d$. The idealized characteristics shown by a solid line in Fig. 7 were obtained by approximating the rapid but continuous movement of the vortex breakdown from midchord to the trailing edge[5] (Fig. 4) by a discontinuous, jump-wise movement. On the right, windward wing half vortex breakdown moves steadily forward toward the apex with increasing roll angle because of the roll-induced decrease of the leading-edge sweep, Eq. (2). The breakdown reaches the apex at $|\phi| \approx 13$ deg, according to the analysis in Ref. 13. The loss of vortex-induced lift on the windward wing half, caused by this forward movement of the vortex breakdown, augments the statically destabilizing data trend generated by the increased vortex-induced lift on the leeward wing half.

Experimental results for a 60-deg delta-wing-body configuration[11] have revealed that when vortex breakdown reaches the apex the moderate suction loads generated downstream of a spiral vortex breakdown are wiped out. This probably accounts for the experimental overshoot by the 65-deg delta wing in Fig. 7 of the idealized characteristics at $\phi_d < \phi < \phi_s$, where $\phi_s \approx 13$ deg. At $\phi > \phi_s$ the windward wing half is completely stalled, contributing negligibly to the rolling moment, whereas the leeward wing half generates the full, statically stabilizing, vortex-induced loading[12] (Fig. 8). This caused the measured rapid decrease of the rolling moment for $\phi > 13$ deg in Fig. 7, resulting in a stable trim point at $\phi_l \approx 20$ deg.

Comparing Figs. 6 and 7, one finds distinct similarities, indicating that the basic flow physics described for the 65-deg delta wing[14] could apply also to the present 45-deg delta wing. From Fig. 6b one obtains the stable trim conditions $\phi_l \approx \pm 55$ deg, which for $\sigma = 30$ deg in Eq. (2) gives $\Lambda_{eff} \approx 71$ deg for the leeward wing half. According to the prediction for sharp-edged delta wings[12] (Fig. 8), this would mean that the contribution to the rolling moment from the leeside wing half is damping. This is also the case for the trim points $\phi_l \approx \pm 55$ deg at $\sigma = 25$ deg (Fig. 6a). Thus, the observed limit-cycle oscillations of the 45-deg delta wing[1] (Fig. 9) cannot be explained through undamping generated by the leeward wing half,

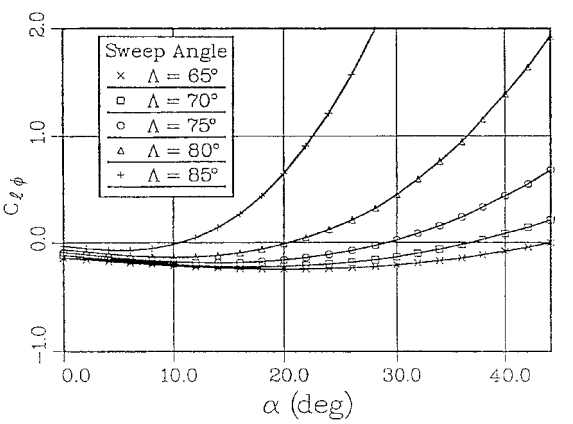

Fig. 8 Effect of leading-edge sweep on the roll damping $C_\ell(\dot{\phi}) = f(\alpha)$ **(Ref. 12).**

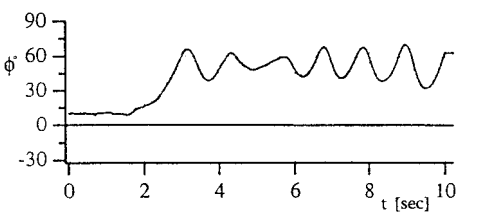

σ = 25 deg

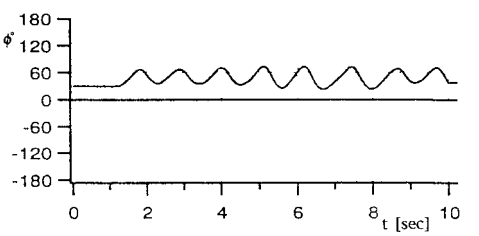

σ = 30 deg

Fig. 9 Roll-angle time history of 45-deg delta-wing model.[1]

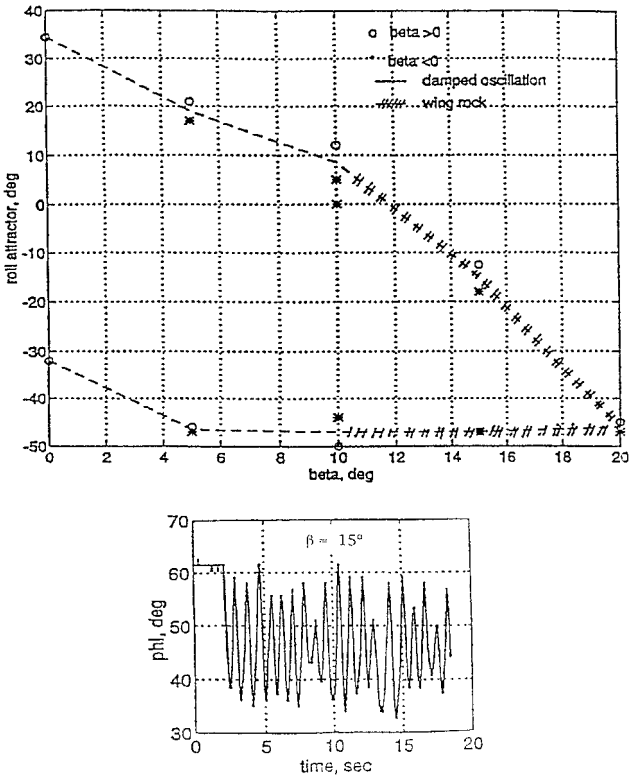

Fig. 10 Measured roll trim angles and roll oscillations for 60-deg delta wing at $\sigma = 30$ deg (Ref. 15).

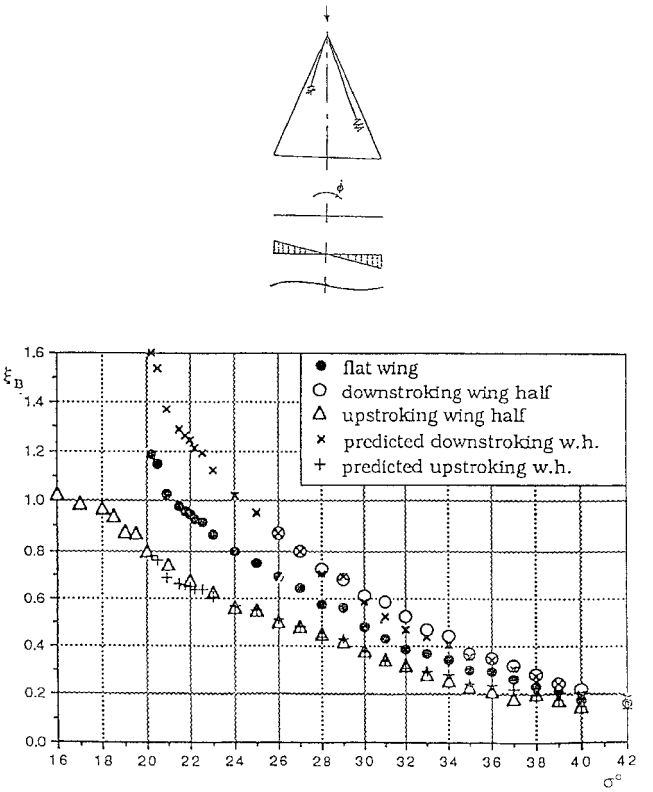

Fig. 11 Effect of spanwise camber corresponding to $K = 0.012$ on vortex breakdown of 65-deg delta-wing-body configuration.[17,18]

which did explain the observed limit-cycle oscillations at $\sigma = 30$ deg and $\beta > 10$ deg observed in experiments with a sharp-edged 60-deg delta wing[15,16] (Fig. 10). There are two possible reasons for these different results, i.e., the moderate leading-edge sweep, 45 deg compared to 60 deg, and/or the difference in leading-edge geometry, large leading-edge radius compared to a sharp leading edge.

It has been demonstrated that the roll-rate-induced camber effect will delay vortex breakdown on the downstroking wing half and promote it on the upstroking side of a sharp-edged 65-deg delta-wing-body configuration[17,18] (Fig. 11). One would expect the roll-rate-induced camber to have a similar effect on part-span leading-edge vortices, i.e., to work toward or against reestablishing the full vortex-induced lift, similarly to the effect of the pitch-rate-induced camber.[19] Thus, the roll-rate-induced camber should generate roll damping for a sharp-edged 45-deg delta wing, and the measured wing rock around $\phi \approx 50$ deg at $\sigma = 25$ and 30 deg (Fig. 9) must have been caused by the rounded leading edge.

For $\sigma = 30$ deg and $\phi = 50$ deg Eq. (2) gives $\Lambda = 21$ deg for the windward wing half. That produces the situation illustrated in Fig. 12. Thus, one needs to analyze the flow over a moderately swept wing leading edge. The effective angle of attack for the leading-edge cross section in Fig. 12 is determined as follows[9]:

$$\alpha_{\text{eff}} = \tan^{-1}(\tan\sigma \cos\phi) \tag{3}$$

For $\sigma = 30$ deg and $\phi = 50$ deg Eq. (3) gives $\alpha_{\text{eff}} \approx 24$ deg. As the AR for the right wing half is 4.00 in Fig. 1 and 4.85 in Fig. 12, α_{eff} is close to the angle for maximum lift $\alpha = 25$ deg in Fig. 2. Thus, during wing rock the right wing half in Fig. 12 would be describing roll oscillations that produce a plunging motion of the rounded leading edge at an angle of attack close to that for maximum lift. When this motion is taking place in the near-stall region, as in the present case, undamping-in-plunge has been measured for airfoils[20] (Fig. 13). The negative damping-in-plunge has been shown to be generated by the moving wall effect on the initial boundary-layer formation near the forward flow stagnation line,[21] as illustrated in Fig. 14. The experimental data trend toward reestablishing damping for $\alpha > 15$ deg in Fig. 13 has the following explanation. The undamping-in-plunge is generated by the moving-wall effect on the

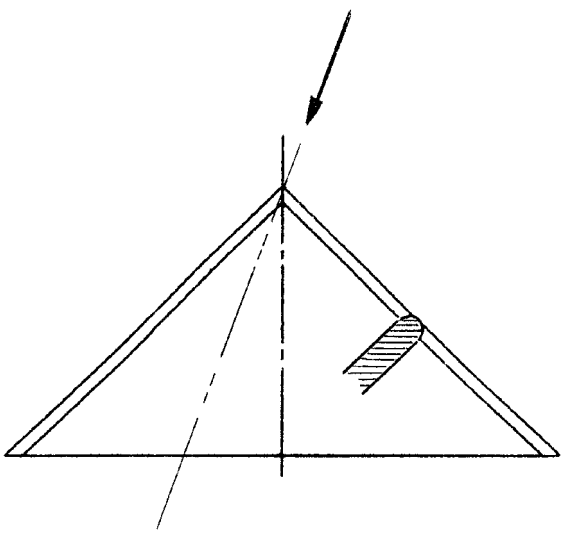

Fig. 12 In-plane flow conditions of 45-deg delta wing at $\sigma = 30$ deg and $\phi = 50$ deg.

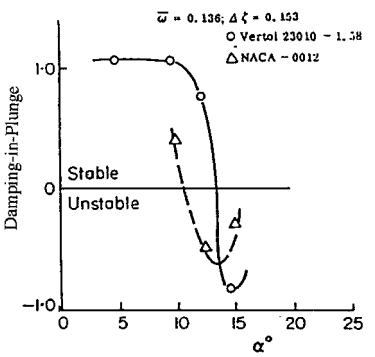

Fig. 13 Measured damping-in-plunge characteristics of airfoils.[20]

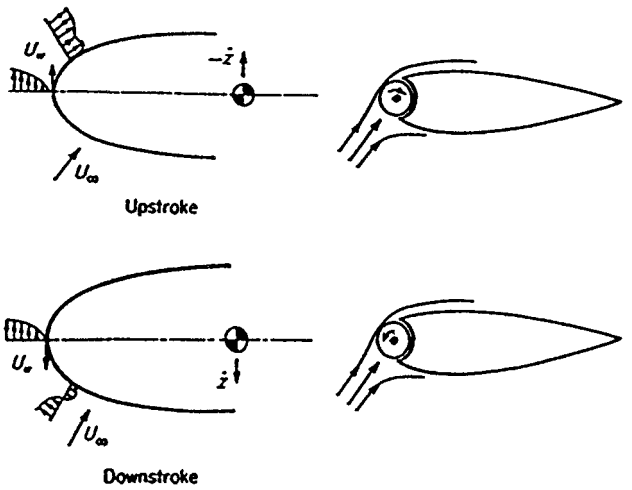

Fig. 14 Moving-wall effect on a pitching or plunging airfoil.[21]

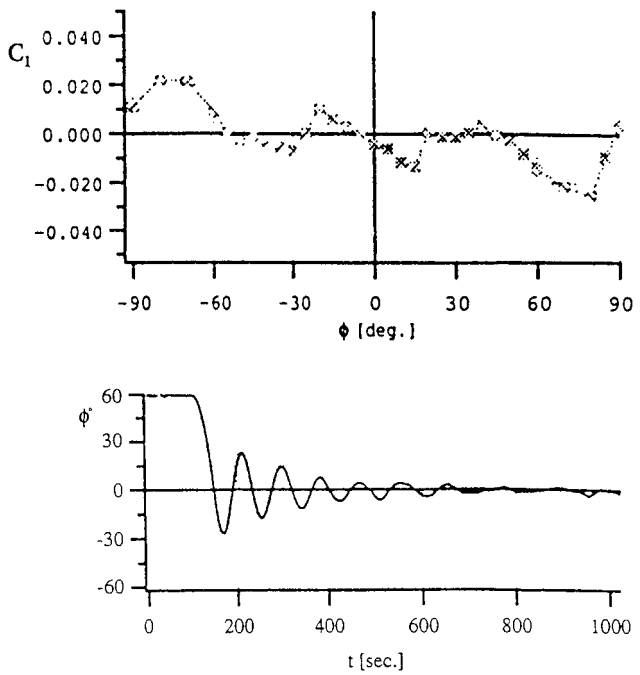

Fig. 15 $C_\ell(\phi)$ and $\phi(t)$ for 45-deg delta-wing model at σ = 35 deg (Ref. 1).

flow separation. Figure 14 illustrates how it will cause attachment of the separated flow during the upstroke, generating a positive normal force, producing undamping at 10 deg $< \alpha <$ 17.5 deg that drives the plunging motion[20] (Fig. 13). During the downstroke, the moving-wall effect promotes flow separation, also generating undamping-in-plunge. At higher angles of attack, certainly beyond $\alpha \approx 20$ deg in Fig. 13, the flow has become totally separated on the leeward side, and only the attached flow on the windward side of the airfoil reacts to the plunging motion, generating damping.

For finite-AR wings the undamping will start at a much higher angle of attack than in the two-dimensional case ($\alpha \approx 10$ deg in Fig. 13).[22] The wing stall at $\alpha \approx 24$ deg (Fig. 2) for the wing in Fig. 12 corresponds to 10 deg $< \alpha <$ 15 deg for the airfoils in Fig. 13. Consequently, one expects the maximum undamping-in-plunge, corresponding to $\alpha \approx 15$ deg in Fig. 13, to occur at $\alpha \approx 30$ deg for the wing in Fig. 12 and last until $\alpha > 34$ deg, corresponding to $\alpha > 17$ deg in Fig. 13. This explains why the oscillations around the trim point at $\phi = 0$ at $\sigma = 35$ deg (Fig. 15) and $\sigma = 45$ deg (Fig. 16) are damped.

The important lesson to be learned from the low-speed results for the thick 45-deg delta wing with a large leading-edge radius[1] is

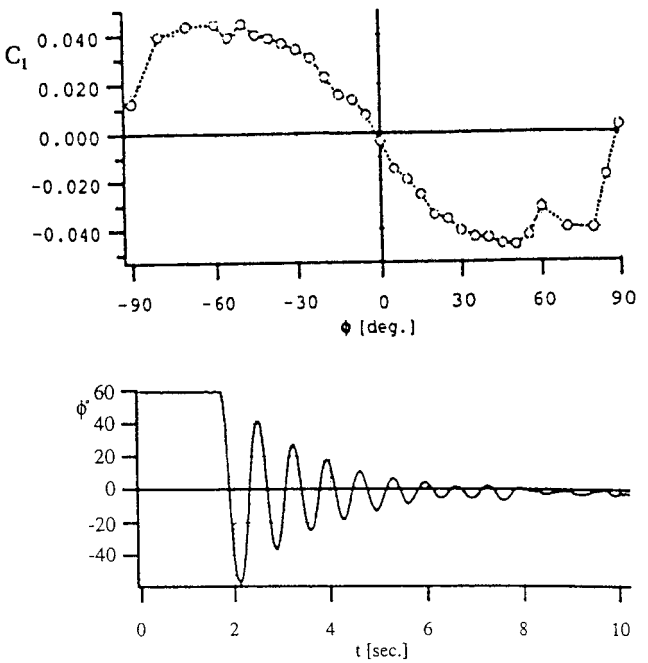

Fig. 16 $C_\ell(\phi)$ and $\phi(t)$ for 45-deg delta-wing model at σ = 45 deg (Ref. 1).

that, because of the large leading-edge radius needed for heat protection, aerospace vehicles with delta-wing planforms of moderate leading-edge sweep will experience nonslender wing rock of the type described in Ref. 22 for straight wings and was experienced by the X-29A aircraft with its 29-deg swept-forward wing.[23]

Conclusions

Analysis of published experimental results shows that wing rock of nonslender delta wings, with leading-edge sweep less than 50 deg, can occur when the following conditions are met:

1) The wing has a rounded leading edge.

2) The inclination of the roll axis is high enough so that during the rolling motion the effective leading-edge sweep and angle of attack of the windward wing half are such that dynamic-stall conditions are produced.

3) Under these conditions there will exist a limited range of the inclination of the roll axis in which the dipping, windward wing half during the rolling motion will experience leading-edge stall of the type observed to cause undamped plunging oscillations of two-dimensional airfoils and wing rock of straight wings. In the present case of a 45-deg delta wing, this resulted in undamped rolling motions, terminating in roll oscillations of the limit-cycle type.

References

[1] Ueno, M., Matsuno, T., and Nakamura, Y., "Unsteady Aerodynamics of Rolling Thick Delta Wing with High Aspect Ratio," AIAA Paper 98-2520, June 1998.

[2] Ericsson, L. E., "Wing Rock Analysis of Slender Delta Wings, Review and Extension," Journal of Aircraft, Vol. 32, No. 6, 1995, pp. 1221–1226.

[3] Jacobs, E. N., and Sherman, A., "Airfoil Section Characteristics as Affected by Variations in the Reynolds Number," NACA TR 586, 1937.

[4] Ericsson, L. E., and King, H. H. C., "Effect of Cross-Sectional Geometry on Slender Wing Unsteady Aerodynamics," Journal of Aircraft, Vol. 30, No. 5, 1993, pp. 793–795.

[5] Wentz, W. H., and Kohlman, D. L., "Vortex Breakdown on Slender Sharp-Edged Wings," Journal of Aircraft, Vol. 8, No. 3, 1971, pp. 156–161.

[6] Cipolla, K. M., and Rockwell, D., "Flow Structure on Stalled Delta Wing Subjected to Small Amplitude Pitching Oscillations," AIAA Journal, Vol. 33, No. 7, 1995, pp. 1256–1262.

[7] Garner, H. C., and Breyer, D. W., "Experimental Study of Surface Flow and Part-Span Vortex Layers on a Cropped Arrowhead Wing," Aeronautical Research Council, R&M 3107, U.K., April 1957.

[8] Hanff, E. S., and Jenkins, S. B., "Large-Amplitude High-Rate Roll Experiments on a Delta and Double Delta Wing," AIAA Paper 90-0224, Jan. 1990.

[9]Ericsson, L. E., and Hanff, E. S., "Unique High-Alpha Roll Dynamics of a Sharp-Edged 65 Deg Delta Wing," Journal of Aircraft, Vol. 31, No. 3, 1994, pp. 520–527.

[10]Ericsson, L. E., "Effect of Angle of Attack on Roll Characteristics of a 65 Deg Delta Wing," Journal of Aircraft, Vol. 34, No. 4, 1997, pp. 573–575.

[11]Bergmann, B., Hummel, D., and Oelker, H.-C., "Vortex Formation over a Close-Coupled Canard-Wing-Body Configuration in Unsymmetrical Flow," AGARD, CP-494, July 1991 (Paper 14).

[12]Ericsson, L. E., and King, H. H. C., "Rapid Prediction of High-Alpha Unsteady Aerodynamics of Slender-Wing Aircraft," Journal of Aircraft, Vol. 29, No. 1, 1992, pp. 85–92.

[13]Jenkins, J. E., Myatt, J. A., and Hanff, E. S., "Body-Axis Rolling Motion Critical States of a 65-Degree Delta Wing," AIAA Paper 93-0621, Jan. 1993.

[14]Ericsson, L. E., "Flow Physics of Critical States for Rolling Delta Wings," Journal of Aircraft, Vol. 32, No. 3, 1995, pp. 603–610.

[15]Pamadi, B. N., Rao, D. M., and Niranjana, T., "Roll Attractor of Delta Wings at High Angles of Attack," International Council of the Aeronautical Sciences, ICAS 94-7.1.2, Sept. 1994.

[16]Ericsson, L. E., "Analysis of the Effect of Sideslip on Delta Wing Roll-Trim Characteristics," Journal of Aircraft, Vol. 34, No. 5, 1997, pp. 586–591.

[17]Ericsson, L. E., and Hanff, E. S., "Further Analysis of High-Rate Rolling Experiments of a 65-Deg Delta Wing," Journal of Aircraft, Vol. 31, No. 6, 1994, pp. 1350–1357.

[18]Huang, X. Z., and Hanff, E. S., "Prediction of Leading-Edge Vortex Breakdown on a Delta Wing Oscillating in Roll," AIAA Paper 92-2677, June 1992.

[19]Ericsson, L. E., "Partial-Span Leading-Edge Vortex Characteristics in High-Alpha Oscillations in Pitch," Journal of Aircraft, Vol. 34, No. 3, 1997, pp. 442–445.

[20]Liiva, J., Davenport, F. J., Grey, L., and Walton, I. C., "Two-Dimensional Tests of Airfoils Oscillating Near Stall," U.S. Army Aviation Labs., TR 68-13, Fort Eustis, VA, April 1968.

[21]Ericsson, L. E., "Moving Wall Effect in Relation to Other Dynamic Stall Flow Mechanisms," Journal of Aircraft, Vol. 31, No. 6, 1994, pp. 1303–1309.

[22]Ericsson, L. E., " Various Sources of Wing Rock," Journal of Aircraft, Vol. 27, No. 6, 1990, pp. 488–494.

[23]Fratello, D. J., Croom, M. A., Nguyen, L. T., and Domack, C. S., "Use of the Updated NASA Langley Radio-Controlled Drop-Model Technique for High-Alpha Studies of the X-29A Configuration," AIAA Paper 87-2559. Aug. 1987.